ResearchGate

See discussions, stats, and author profiles for this publication at: https://www.researchgate.net/publication/301894695

Double resonance effect in Daeheuksando Port caused by air pressure disturbances in Yellow Sea on March 31, 2007

Conference Paper *in* Journal of Coastal Research · March 2016

DOI: 10.2112/SI75-229.1

CITATIONS
8

READS
149

6 authors, including:



Myung-Seok Kim
Korea Polar Research Institute (KOPRI)
22 PUBLICATIONS **91** CITATIONS
SEE PROFILE



Hyunsu Kim
Korea Power Exchange
46 PUBLICATIONS **127** CITATIONS
SEE PROFILE



Bon-Ho Gu
Korea Institute of Ocean Science & Technology (KIOST)
9 PUBLICATIONS **29** CITATIONS
SEE PROFILE



Seung Buhm Woo
Inha University
108 PUBLICATIONS **874** CITATIONS
SEE PROFILE

All content following this page was uploaded by Hyunsu Kim on 06 May 2016.

The user has requested enhancement of the downloaded file.

Journal of Coastal Research	SI	75	1142 - 1146	Coconut Creek, Florida	2016

Double Resonance Effect at Daeheuksando Port Caused by Air Pressure Disturbances in Yellow Sea on 31 March 2007

Myung-Seok Kim[†], Hyunsu Kim[‡], Yoo-Keun Kim[‡], Bon-Ho Gu[†], Ho-Jae Lee[‡], and Seung-Buhm Woo[†*]

[†]Department of Ocean Science,
College of Natural Sciences, Inha University,
Incheon, South Korea

[‡]Department of Atmospheric Science,
Pusan National University,
Busan, South Korea

www.cerf-jcr.org

www.JCRonline.org

ABSTRACT

Kim, M.S.; Kim, H.S.; Kim, Y.K.; Gu, B.H.; Lee, H.J., and Woo, S.B., 2016. Double resonance effect at Daeheuksando Port caused by air pressure disturbances in Yellow Sea on 31 March 2007. *In:* Vila-Concejo, A.; Bruce, E.; Kennedy, D.M., and McCarroll, R.J. (eds.), *Proceedings of the 14th International Coastal Symposium* (Sydney, Australia). *Journal of Coastal Research*, Special Issue, No. 75, pp. 1142 - 1146. Coconut Creek (Florida), ISSN 0749-0208.

We found that an internal resonance, combined with other topographic effects, following an external resonance could significantly amplify insignificant sea-level oscillations in the open sea to wave heights of several meters in a coastal area. Sudden sea-level oscillations characterized by high frequencies (0.0042-0.5 min^{-1}) and a maximum wave height of about 1 m were observed at Daeheaksando Port (DP) on 31 March 2007. These sea-level oscillations, which caused heavy casualties and large economic loss, were also detected along the west coast of South Korea. Particularly, at DP, there were sea-level oscillations that had significant power spectrum in a specific period band. When the maximum power spectrum of the sea-level oscillations increased rapidly, the period of the maximum power spectrum converged toward the fundamental period of the port. However magnitude of the air pressure disturbance at DP could not make such sea-level oscillations. The resulting sea-level oscillations were likely amplified by the free waves generated by air pressure disturbances at KyukRyulbeedo (KR) and propagated to DP. The initial magnitude of the disturbances propagated from Shandong was approximately 2.5 hPa/10-min, based on results of the atmospheric model. Theoretically, a 2.5 hPa air pressure change can make sea-level oscillations of about 2.5 cm, but it made meteotsunamis in the port because of the double resonance effect on 31 March 2007.

ADDITIONAL INDEX WORDS: *Air pressure disturbances, meteotsunamis, double resonance effect.*

INTRODUCTION

Severe damage was caused at around 0000 KST on 31 March 2007 by an abnormal wave that occurred in Yellow Sea. "Abnormal wave" is a term that has been used in South Korea to describe the characteristics of a meteotsunami, which can generate sudden and very large waves near the coast like a tsunami. According to reports from the Korea Meteorological Administration (KMA), the meteotsunamis that occurred on 31 March 2007 caused a total of six human casualties (four dead and two injured) and property damage estimated at up to two million dollars, including flooded homes, capsized fishing boats, and losses of fish farm (Yoon and Eom, 2013).

Meteotsunamis associated with atmospheric instability were known in some countries as "abiki" in Japan, "rissagga" in Spain, "šćiga" in Croatia, "marrubbio" in Sicily, "milghuba" in Malta, "seebär" in Baltic coutries, "death waves" in Western Ireland and "inchas" in the Azores and Madeira islands (Vilibić *et al.*, 2014). The general mechanism of a catastrophic meteotsunami, according to the diagram suggested by Monserrat *et al.* (2006), is as follows.

(1) A small air pressure disturbance (3 hPa) over a short time interval that initially propagates from the open sea causes sea-level oscillations of approximately 3 cm due to the inverted barometer effect. (2) Then, as the phase speed of the propagating sea-level oscillations and the speed of air pressure disturbance become similar, Proudman resonance, which is an external resonance, occurs at the air-sea interface. The resonance amplifies the amplitude and lengthens the wavelength of the sea-level oscillations. (3) The amplitude of the propagating sea-level oscillations can increase again at the shelf region due to topographic properties. (4) Wave deformations near an inlet or artificial structure can also cause significant sea-level oscillations. When the period of the sea-level oscillations entering the harbor corresponds with the fundamental period of the harbor, harbor resonance, which is an internal resonance, occurs (1-5 m). The risk of the destructive meteotsunami is closely related to the shelf topography and coastline geography, which create a "double resonance effect" (Rabinovich, 1993) that is a combination of the resonances.

The generation of air pressure disturbances that resulted from atmospheric gravity waves that repeatedly propagated toward the west coast of South Korea produced meteotsunamis on 31 March 2007 (Choi *et al.*, 2008). During the meteotsunamis, both the air pressure disturbances and high frequency sea-level oscillations propagated in a south-easterly direction (Eom *et al.*, 2012). By applying crests of the air pressure disturbances derived from 3 hourly weather charts to a 2-dimensional shallow water wave model, they simulated sea-level oscillations amplified by the Proudman resonance effect. Kim *et al.* (2014)

DOI: 10.2112/SI75-229.1 received 15 October, 2015; accepted in revision 15 January, 2015.
*Corresponding author: sbwoo@inha.ac.kr
©Coastal Education and Research Foundation, Inc. 2016

showed that atmospheric instability, generated by the passing of a low pressure system accompanying a cold front, propagated across the Yellow Sea from Shandong (Figure 1) from the results of a synoptic analysis and the Weather Research and Forecast model (WRF).

In this study, we investigated the presence of harbor resonance after Proudman resonance and the degree of amplification due to each resonance at DP on 31 March 2007.

METHODS

Mean sea-level pressure at KR and DP at an interval of a 1-min was used for the analysis of the meteotsunamis that occurred at DP on 31 March 2007. Radar images that could show the evolution of atmospheric instability over the Yellow Sea at an interval of a 10-min were also used. These atmospheric data were provided by KMA. The tide level at DP at an interval of a 1-min was provided by the Korea Hydrographic and Oceanographic Administration (KHOA).

In general, signals in the time domain due to meteotsunamis are characterized by localized peaks at the specific time and are attenuated non-periodically. In order to analyze such non-stationary signals, the wavelet transform, which uses an isolated wave as a basis function, was used. Because time series can be converted into time–frequency domain through the wavelet transform, it is possible to analyze how the variability of interest changes with time and frequency. The Morlet wavelet was used as the wavelet basis function because the wavelet scale is almost equal to the Fourier period. To estimate power spectrum of tide level in the high frequency band during meteotsunamis, wavelet reconstruction and Scale Averaged Wavelet Power (SAWP) were used (Torrence *et al.*, 1997).

The Advanced Research WRF version 3.6.1 was used to simulate the atmospheric instability. To simulate fine air pressure at the lowest level in WRF, dense sigma levels and two nested domains were used. The grid information of each domain and the physical options of the model integration are shown in the Table 1. FNL (Final) Operational Global Analysis data, which are reanalysis data from the Global Forecast System (GFS), National Centers for Environmental Prediction (NCEP), and Real Time Global SST were used as initial boundary conditions. A total of 6 days, from 0900 KST on 27 March 2007 to 0900 KST on 02 April 2007, was simulated. Considering the spin-up time of 1 day, only the results for last 5 days were used.

Table 1. *Details of the grids and the physics options used in the WRF model (Kim et al., 2014)*

Scheme	Domain 1	Domain 2	Domain 3
Horizontal grid	165×150	271×226	289×307
Resolution	30 km	10 km	3.3 km
Vertical grid	48 layers (sigma coordinate)		
Microphysics	WSM3	Milbrandt-Yau 2-Moment	
Surface layer	Revised MM5		
Land Surface	Noah-LSM		
Boundary layer	YSU		
Cumulus	Kain-Fritsch		
Longwave radiation	RRTMG		
Shortwave radiation	RRTMG		

RESULTS

The results section is organized into three subsections. To explain the double resonance effect at DP, the organization is sea-level oscillations at the port, source of meteotsunamis, and evidence of harbor resonance in sequence.

Characteristics of sea-level oscillations at DP

There was mainly a dominant power spectrum at the diurnal and the semi-diurnal tidal cycle in the tide level of DP during 31 March 2007 and 01 April 2007 (Figure 2a and 2b). Additionally, in a short period of less than 4-h, sea-level oscillations similar to tsunami oscillations existed due to the meteotsunamis. As shown in the wavelet scalogram, the power spectrum of the tides distributed above 10^5 cm^{2}min and the power spectrum of the meteotsunamis distributed within 10^2 cm^{2}min and 10^5 cm^{2}min. In addition, sea-level oscillations with amplitude less than 30 cm also occurred before and after 31 March, the day on which human casualties and property damage were reported. As shown in Figure 2c, the maximum SAWP of the residual tide level (less than 4-h) occurred at 0056 KST on 31 March 2007 during high tide, indicating that the arrival time of the meteotsunamis. Subsequent disturbances occurred repeatedly after this time, and sea-level oscillation lasted approximately 18-h (Figure 2, gray dashed line). It is well known that meteotsunamis on 31 March first occurred at the tidal station near KR before reaching DP on 31 March (Eom *et al.*, 2012).

Air pressure disturbances propagated from Shandong

To understand the rapid evolution of air pressure disturbances in space and time, atmospheric pressure at an interval of a 1-min from the model results was analyzed.

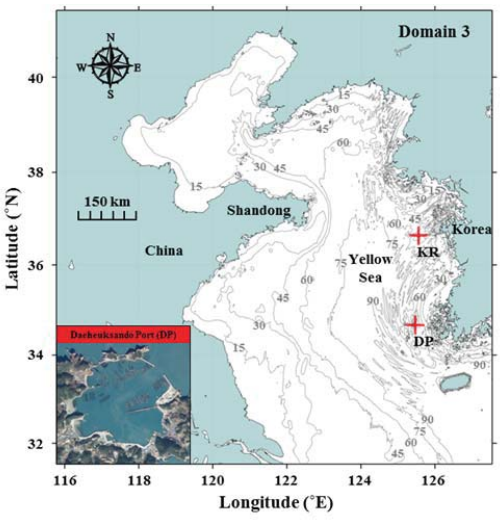


Figure 1. Study area (Domain 3) and satellite image of DP captured from Google Earth. Red cross markers indicate locations of KR and DP. Gray dashed lines are bathymetric contours.

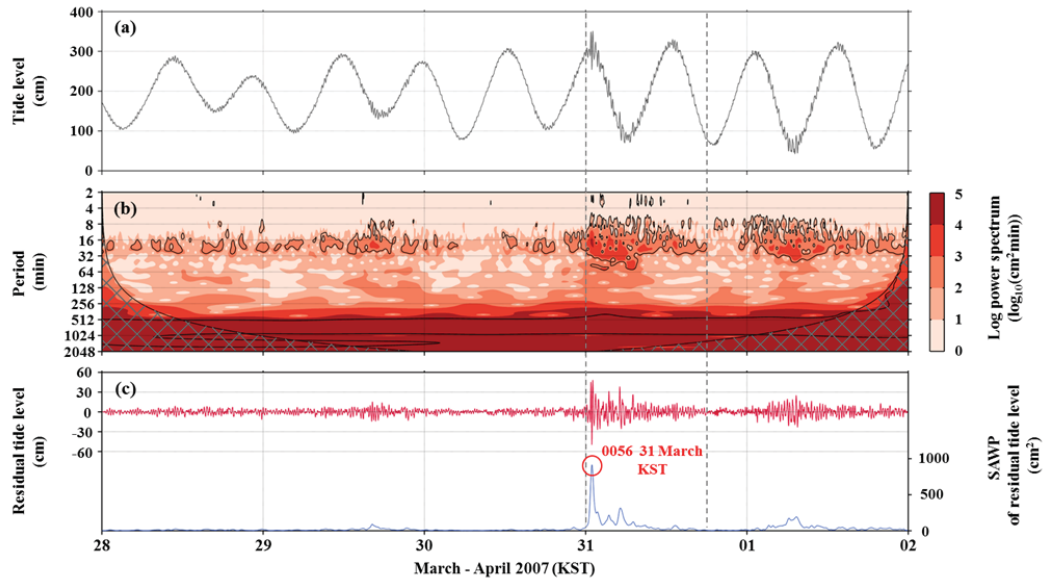


Figure 2. Tide level, wavelet scalogram of the tide level, and residual tide level (high pass filtered, 4-h) and Scale Averaged Wavelet Power (SAWP) of the residual tide level at DP. (a) Gray dashed lines indicate the time interval of occurrence of successive accidents. (b) The left axis is Fourier period (min). The thick contour encloses regions of greater than 95% confidence level for the power spectrum of tide level during the five days. Cross-hatched regions indicate the cone of influence, where edge effects become important. (c) Red circle indicates arrival time of meteotsunami.

The first air pressure disturbance at Shandong (Figure 3a, P0), which had a significant diameter of approximately 400 km at 2100 KST on 30 March, gradually developed into a wave crest line as it propagated (Figure 3b, P0). Then, at 0000 KST on 31 March, two wave crest lines divided from the initial P0, and P1 and P2 moved successively in an eastern direction toward the west coast of South Korea (Figure 3c, P1 and P2). At this time, the radar images indicated a high rain rate which is a sign of the atmospheric instability also propagated while showing a spatio-temporal distribution that was similar to the simulated air pressure disturbances (Figure 3e-3g). However, it was impossible to identify the location of P0 that appeared on the model with the radar images because of the limited coverage of the radar. Additionally, the air pressure disturbances derived from the model results tend to dissipate quickly at the west coast (Figure 3d and 3h).

The amplitude of the air pressure disturbance near Shandong was approximately 2.5 hPa/10-min at the maximum amplitude (Figure 3a, P0). The slopes of the wave crest lines (Figure 3c, P1 and P2) were 62˚ and 77˚ (clockwise from the northward direction), respectively, and the two wave crest lines propagated together in an eastward direction from 2230 KST on 30 March to 0330 KST on 31 March at an average speed of 28 m/s. Especially, they propagated by passing through the regions between KR and DP (Figure 3c and 3d). Considering the spatial scale of the wave crest lines, it can be assumed that the sea-level oscillations lasted for a long time because of the influence of P2 rather than P1 (Figure 3c). However, the critical meteotsunami was reported during propagation of P1, and the sea-level oscillations resulting from P1 had much more SAWP than those from P2 (Figure 2c, blue line).

Harbor resonance at DP

Air pressure disturbance was derived from the sea-level pressure at KR and DP to analyze the cause of the sea-level oscillations detected at DP. As a result, only insignificant air pressure disturbance (Figure 4a, bottom gray line) was examined at DP where meteotsunamis occurred. However, air pressure disturbance at KR (Figure 4a, bottom red line) was more significant (-4.1-3.0 hPa/10-min) during P1. Thus, it could be concluded that maximum power spectrum (10^3-10^4 cm^{2}min) at DP during P1 (Figure 4b), black line) resulted from the free waves propagated from KR because the magnitude of the air pressure disturbance that occurred at DP could not generate such sea-level oscillations. Similarly, the maximum power spectrum during P2 was also increased rapidly by the propagated sea-level oscillations originated from KR. After P1 and P2, the air pressure disturbance that occurred at DP increased up to 1.7 hPa/10-min at 0720 KST on 31 March, but power spectrum of the sea-level oscillations did not increase as sharply as before. It seemed that such air pressure disturbance at DP occurred because of the influence of the P2 wave crest line, which was elongated as shown in Figure 4d.

Before meteotsunamis arrived at DP almost until 0000 KST on 31 March, the period of the maximum power spectrum occurred near the cut-off frequency (Figure 4b, blue line). However, the period converged into a specific period band

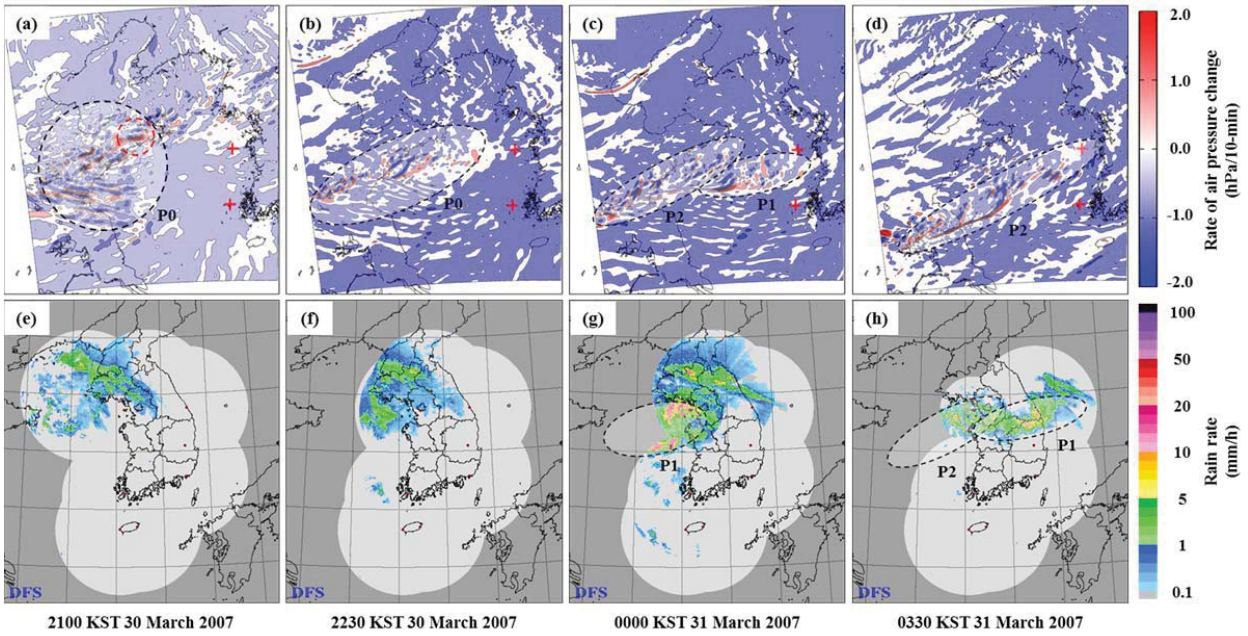


Figure 3. Horizontal distribution of the air pressure disturbances at the bottom layer derived from WRF 1-min interval results by using rate of air pressure change (Šepić and Vilibić, 2011) and radar images. P0, P1, and P2 indicate evolution of the atmospheric instability associated with pressure disturbances. Red cross markers indicate location of KR and DP (a-d).

when the maximum power spectrum increased (Figure 4b, red dashed line). Even after P1 and P2 passed, sea-level oscillations that exceeded the maximum power spectrum ranging from 10^2 cm^{2}min to 10^3 cm^{2}min in the same period band lasted until 1800 KST on 31 March. It was considered as continuing harbor resonance during and after meteotsunamis.

DISCUSSION

The rate of air pressure change derived from the air pressure in the model results was utilized to estimate the amplitude of sea-level oscillations that were amplified by the external resonance from Shandong. According to Proudman (1929), the resonance shown by the following formula occurs if the speed of air pressure disturbances propagated from open sea equals the longwave phase speed of ocean waves.

$$\Delta\eta = \Delta\eta^*/\left(1 - F_r{}^2\right), \quad (1)$$

where $\Delta\eta$ is the amplified amplitude in open ocean, $\Delta\eta$ = -$\Delta P_a/\rho g$, where ΔP_a is the air pressure disturbance and ρ is the water density, and F_r is the Froude number. Considering the average velocity of P1 (28 m/s) and the depth range of the Yellow Sea (60-90 m) from Shandong to DP, the range of the Froude number was calculated to be between 0.9 and 1.2, which is a favorable condition for meteotsunami. When the amplified amplitude by Proudman resonance is calculated by using (1), the $\Delta\eta$ caused by the resonance approaches infinity if F_r = 1. Thus, the amplified amplitude was calculated by using (2), which was suggested by Hibiya and Kajiura (1982).

$$\Delta\eta = -\Delta\eta^* x_f/2L_1, \quad (2)$$

where L_1 is the width of an air pressure disturbance in its direction of propagation and x_f is the distance from the source area. The red dashed circle in Figure 3a represents the maximum magnitude of the air pressure disturbance (2.5 hPa/10-min) located at Shandong. The model results ($\Delta\eta^*$ = 2.5 cm, L_1 = 33 km, x_f = 320 km) were utilized with an assumption that the amplitude of the sea-level oscillation due to the air pressure disturbance would be approximately 2.5 cm based on the inverted barometer effect. Therefore, $|\Delta\eta|$ was 12.2 cm, which is 4.9 times the amplitude of $|\Delta\eta^*|$.

The fundamental period of DP was estimated from the spatial information in order to analyze the cause of the significant power spectrum at DP, which was frequently amplified in a specific frequency band after Proudman resonance. Basin's empirical formula of the fundamental period for a semi-elliptic geometry (Wilson, 1972), which is most similar to the geometric type of DP is given by

$$T_0 = 2.220[2L/(gh_1)^{1/2}], \quad (3)$$

where L is the length of the port, h_1 is the depth at the open mouth of the port, and g is gravitational acceleration. When the spatial information of DP was applied to (3), T_0 was calculated to be in the range between 14.3-min and 18.9-min (L = 1600 m, h_1 = 4-7 m). This implies that there was harbor resonance at DP because the range of the calculated T_0 approximated to the period band between 16-min and 32-min

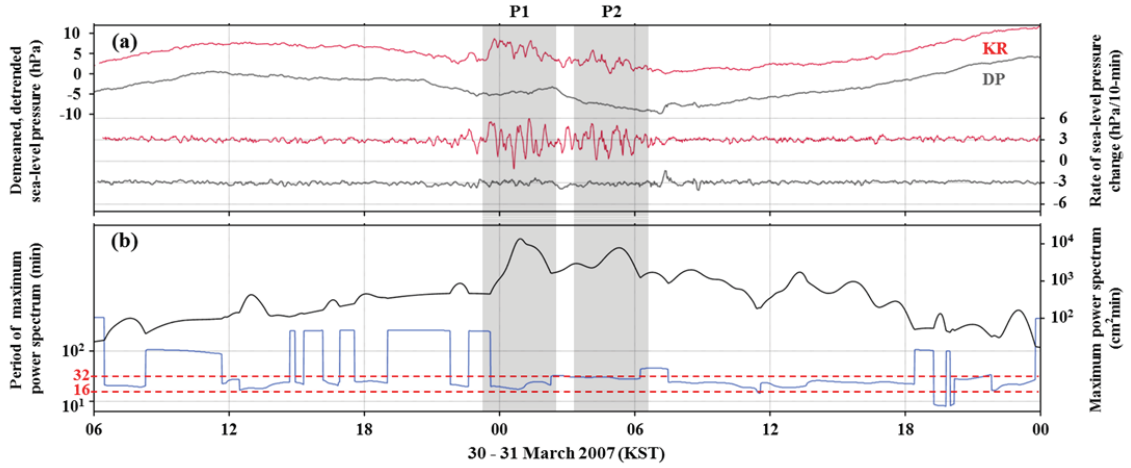


Figure 4. The evidence of harbor resonance at DP. (a) Demeaned, linearly detrended sea-level pressure (top) and rate of sea-level pressure (bottom) at KR (red line) and DP (gray line). Gray boxes indicate duration of the atmospheric instabilities (P1, P2). (b) Maximum power spectrum of the residual tide level (black line) and period of the maximum power spectrum (blue line). Red dashed lines indicate convergence to the specific period band when the maximum power spectrum increases.

whenever the maximum power spectrum increased suddenly (Figure 4b). Excluding the amplified amplitude caused by the external resonance from the initial amplitude (49.7 cm) when the meteotsunami first arrived at DP, approximately 75.5% (37.5 cm) of the amplitude was amplified by the internal resonance combined with other topographic effects.

CONCLUSIONS

In this work, we found that sea-level oscillations with amplitude of 2.5 cm that occurred in the open sea were amplified 20 times at DP by the harbor resonance succeeding Proudman resonance, when including the topographic effect. Therefore, the meteotsunamis at DP that occurred on 31 March 2007 were a phenomenon caused by the double resonance effect, which is the combination of an external resonance and an internal resonance. Further quantitative research using an atmosphere-ocean coupled model should be conducted to better understand how the sea-level oscillations that propagate with the air pressure disturbances evolve with time and how much they can be amplified by the resonances.

ACKNOWLEDGMENTS

This work was funded by the Korea Meteorological Administration Research and Development Program under Grant KMIPA 2015-1071.

LITERATURE CITED

Choi, B.J.; Park, Y.W., and Kwon, K.M., 2008. Generation and growth of long ocean waves along the west coast of Korea in March 2007. *Ocean and Polar Research*, 30(4), 453-466.

Eom, H.M.; Seung, Y.H.; Woo, S.B., and You, S.H., 2012. Analysis of abnormal wave at the west coast on 31 March 2007. *Journal of Korean Society of Coastal Ocean Engineers*, 24(3), 217-227.

Hibiya, T. and Kajiura, K., 1982. Origin of Abiki phenomenon (a kind of seiches) in Nagasaki Bay. *Journal of the Oceanographical Society of Japan*, 38, 172-182.

Kim, H.S.; Kim, Y.K.; Woo S.B., and Kim, M.S., 2014. Atmospheric analysis on the meteotsunami case occurred on 31 March 2007 at the Yellow Sea of South Korea. *Journal of Environmental Science International*, 23(12), 1999-2014.

Monserrat, S.; Vilibić, I., and Rabinovich, A.B., 2006. Meteotsunamis: atmospherically induced destructive ocean waves in the tsunami frequency band. *Natural Hazards Earth System Sciences*, 6, 1035-1051.

Proudman, J., 1929. The effects on the sea of changes in atmospheric pressure, *Geophysical Journal International*, 2(4), 197-209.

Rabinovich, A.B., 1993. Long Ocean Gravity Waves: Trapping, Resonance, and Leaking (in Russian). *St. Petersburg: Gidrometeoizdat*, 325p.

Šepić, J. and Vilibić, I., 2011. The development and implementation of a real-time meteotsunami warning network for the Adriatic Sea. *Natural Hazards and Earth System Sciences*, 11, 83-91.

Torrence, C. and Compo, G.P., 1998. A practical guide to wavelet analysis. *Bulletin of the American Meteorological Society*, 79, 61-78.

Vilibić, I.; Monserrat, S., and Rabinovich, A.B., 2014. Meteorological tsunamis on the US East Coast and in other regions of the World Ocean. *Natural Hazards*, 74, 1-9.

Wilson, B., 1972. Seiches. *Advances in Hydroscience*, 8, pp. 1-94.

Yoon, J.H. and Eom, H.M., 2013. Challenge to no casualty of the abnormal waves at the west coast of South Korea. *Seoul, South Korea: Observation Infrastructure Bureau of Korea Meteorological Administration*, 3p.

View publication stats